PHYSICAL REVIEW B VOLUME 46, NUMBER 11 15 SEPTEMBER 1992-I

Strong resonances in core-level photoemission

G. van der Laan
Science and Engineering Research Council, Daresbury Laboratory, Warrington WA4 4AD, United Kingdom

B. T. Thole
Materials Science Centre, University of Groningen, 9747 AG Groningen, Netherlands

H. Ogasawara and Y. Seino
Department of Physics, Faculty of Science, Tohoku University, Aoba-ku, Sendai 980, Japan

A. Kotani
Institute for Solid State Physics, University of Tokyo, 7-22-1 Roppongi, Minato-ku, Tokyo 106, Japan
(Received 18 June 1992)

We predict very strong peak enhancements in core-level photoemission at the resonance with a deeper core-level absorption. This allows a straightforward interpretation of core-level spectroscopy in two ways: (a) photoemission peaks can be resolved in resonance with different x-ray absorption peaks, and (b) x-ray absorption peaks can be resolved using partial electron yield at constant binding energy. This can be used to study covalency effects in transition-metal, rare-earth, and actinide compounds. An example is given for nickel metal using a cluster calculation including multiplet structure.

Resonant photoemission is a well-known technique based on the effect that the valence-band photoemission is enhanced by a super-Coster-Kronig decay after photon excitation at a shallow core-level absorption edge.[1] At such edges the direct and resonant photoemission are of the same order of magnitude, resulting in complicated interference effects that can be used in the analysis of the spectrum. However, the recent progress in high-resolution monochromators for the soft x-ray region allows access of deeper core levels, where the ratio of the cross section for x-ray absorption to that of direct photoemission is much larger, producing an enhancement of 2 orders of magnitude. The interference between the two channels is then negligible, allowing a much more straightforward analysis. This opens the field of resonant photoemission, with its greatly increased detail of information, to use as a standard tool for nonspecialists. The strong enhancement has recently been demonstrated for the valence-band photoemission in CuO at resonance with the Cu $2p$ absorption.[2] In this paper, we show that at these deeper core-hole resonances the enhancement is so strong that it can be used to interpret very small satellite structures in core-level spectra.

Core-level spectroscopy is applied routinely in the study of covalent mixing in $3d$ transition-metal, rare-earth, and actinide compounds.[3] Its strong point is that due to the electrostatic core-valence interactions the different final-state configurations are separated in energy and display characteristic multiplet structures. The number of parameters needed for a detailed analysis requires the combined information of several core-level spectroscopies, such as x-ray absorption (XAS), x-ray photoemission (XPS), and Auger. However, the different numbers of holes in the final states produced by these methods introduce new uncertainties, hampering a direct comparison. Therefore, important problems remain unsolved, such as whether peak splittings are due to configuration interaction or exchange interaction. Resonant core-level spectroscopy gives the advantage that the photoemission and x-ray absorption are combined in a single analysis. Despite energy shifts and multiplet splitting the common origin of related peaks in the two spectra can be deduced directly by qualitative reasoning without complete calculations. The technique is element selective in the photon energy as well as in the binding energy.

Consider an x-ray absorption transition $v^n \rightarrow \underline{c}_1 v^{n+1}$, where an electron is excited from a core level c to a valence level v (underlined levels contain a hole). When there is an attractive Coulomb interaction between the core hole and the valence electrons the excited state is localized, i.e., it is below the continuum levels $\underline{c}_1 v^n k_\epsilon$. Neglecting fluorescence, which is small for not too deep core levels, the excited state decays by Auger transitions. The accessible final-state configurations are $\underline{c}_2\underline{c}_3 v^{n+1}\epsilon_l$, $\underline{c}_2 v^n \epsilon_l$, and $v^{n-1}\epsilon_l$, where ϵ_l is an electron in a continuum state. The latter two configurations can also be reached by direct photoemission, which gives rise to interference effects. The photoemission intensities are determined by the fractional parentage of the ground state to the final states, whereas the photoabsorption decay is governed by the Auger matrix elements.

The importance to covalent materials becomes immediately clear for a $3d$ transition-metal compound with a mixed (hybridized) ground state where both the $2p$ absorption and $3p$ photoemission have distinct multiplet and satellite structures due to the Coulomb interactions involved. In this case the $2p3p3d$ decay channel is $d^n + d^{n+1} \rightarrow \underline{2p}d^{n+1} + \underline{2p}d^{n+2} \leftrightarrow \underline{3p}d^n + \underline{3p}d^{n+1}$, where the photoemission only comes from the specific absorption levels selected by the photon energy chosen.

We illustrate the power of resonant core-hole photoemission by the example of nickel, where it can be used to

 ©1992 The American Physical Society

investigate the character of the ground state. In a localized model the ferromagnetism of nickel metal arises from a small d^8 weight. The lowest state of this configuration, the triplet state, imposes a spin alignment with adjacent Ni atoms by fluctuation between d^9+d^9 and d^8+d^{10}. However, the photoemission satellites arising from the d^8 contribution are weak and they overlap with those arising from d^9. Although at the resonance of the $3p$ absorption edge the satellite structure in the valence-band photoemission is enhanced, its intensity is still lower than that of the main peak. The satellites are even weaker in XAS, where the effect of the core hole is small due to the additional d electron. However, circular magnetic x-ray dichroism (CMXD) has recently provided evidence for the presence of d^8 character in the ground state.[4]

For the resonance at the $2p$ edge we performed calculations of the x-ray absorption and photoemission spectra using a cluster calculation in spherical symmetry, without $3d$ spin-orbit coupling, including multiplet effects.[5] A ground state with weights of 14.3% d^8, 48.1% d^9, and 37.6% d^{10} gives a good agreement with experimental photoemission[6] and x-ray absorption data.[7]

The upper curve in Fig. 1 shows the calculated $2p_{3/2}$ absorption spectrum composed of the dipole transitions to the excited states. The main peak has primarily $\underline{2p}3d^{10}$ character and the barely visible satellite structure at 4–6.5 eV higher energy has predominantly $\underline{2p}3d^9$ character with high spin at the low-energy side, and low spin at the high-energy side. A linewidth of 0.285 eV half width at half maximum (HWHM) is due to Auger decay. Table I gives all possible decay channels with their contributions to the $2p_{3/2}$ core-level width.

Figure 2 shows the $3p$ photoemission and the $2p3p3d$ decay.[8] The off-resonance intensity $I(E_0)$ consists of a leading peak with primarily $\underline{3p}d^{10}$ character and satellite structures with $\underline{3p}d^9$ and $\underline{3p}d^8$ character. The large $3p$-$3d$ electrostatic interaction splits the $\underline{3p}d^9$ state into three distinguishable peaks with $^3F+{}^1D$, $^3P+{}^3D$, and $^1P+{}^1F$ symmetry. The $\underline{3p}d^{10}$ final state cannot resonate, but the $\underline{3p}d^9$ and $\underline{3p}d^8$ final states can be reached by decay from $\underline{2p}d^{10}$ and $\underline{2p}d^9$, respectively. The other curves in Fig. 2 show the photoemission intensity at the photon energies E_m and $E_{s1,2}$ corresponding to the main and satellite absorption peaks, respectively, given in Fig. 1. Knowing that these peaks correspond to $\underline{2p}d^{10}$ and $\underline{2p}d^9$, respectively, we see immediately that the peaks in the middle of the photoemission spectrum must be $\underline{3p}d^9$ because they are apparently formed by decay of the $\underline{2p}d^{10}$ states produced at E_m. The higher binding energy peaks, but also hidden structure in the middle of the photoemission spectrum, are enhanced at E_{s1} and E_{s2}, and are therefore $\underline{3p}d^8$. The lowest binding-energy peak hardly resonates, confirming its $\underline{3p}d^{10}$ character. This nonresonant behavior is of course particular to $\underline{3p}d^{10}$ and

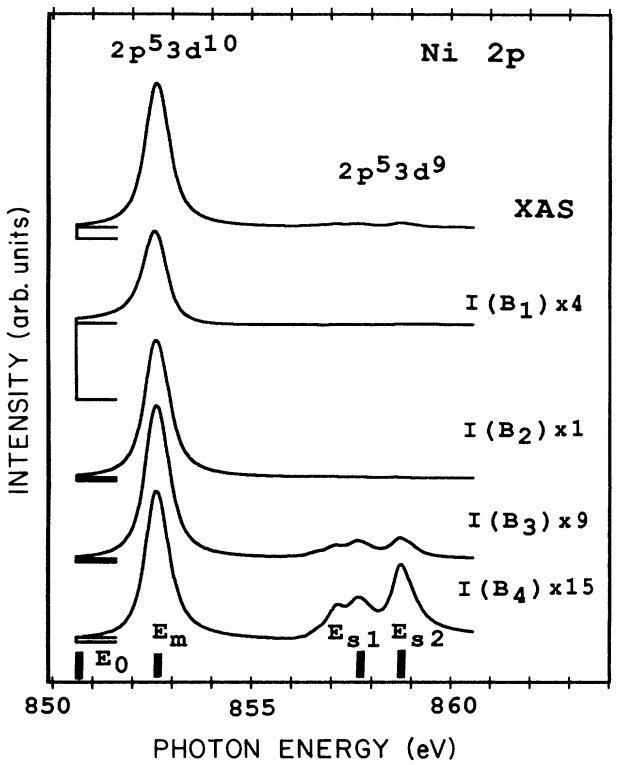

FIG. 1. Calculated Ni $2p_{3/2}$ absorption spectrum (XAS) and the $2p3p3d$ CIS spectra corresponding to the binding energies B_1, B_2, B_3, and B_4 given in Fig. 2. The direct photoemission contribution is shown on the left side. E_0 (off-resonance), E_m (main peak), and E_{s1} and E_{s2} (satellites) indicate the photon energies of the photoemission spectra in Figs. 2 and 3.

does not occur for other configurations. However, a small enhancement due to some $\underline{3p}d^9$ character is detectable. A complication is the fact that also $^3F+{}^1D$ does not resonate, showing that although resonant enhancement is a great help in analyzing spectra, calculations or comparison to spectra of other compounds containing the same element are still useful.

Figure 3 shows the $3s$ photoemission together with the $2p3s3d$ (Ref. 9) and $2p3p3p$ (Ref. 10) resonant decays. In the direct photoemission $I(E_0)$ the main peak has $3sd^{10}$ character, whereas the satellite has mainly $3sd^9(^{3,1}D)$ character. This peak separation is not due to the exchange splitting of the $3s$ level by the valence band (c.f. van Acker *et al.*[11]). At E_m, the $3sd^9$ peak and the $3p^4d^{10}$ structure, which is split into a ^3P, ^1D, and ^1S state, are enhanced. Although the $2p3p3p$ decay does not in itself interfere with direct photoemission, the two possible ^1D final states in $3p^4d^{10}$ and $3p^4d^9$ have configuration

TABLE I. Contributions to the Auger HWHM width of the Ni $2p_{3/2}$ absorption level.

Decay	$2p3s3s$	$2p3s3p$	$2p3s3d$	$2p3p3p$	$2p3p3d$	$2p3d3d$
Γ (meV)	1	4	6	80	86	108

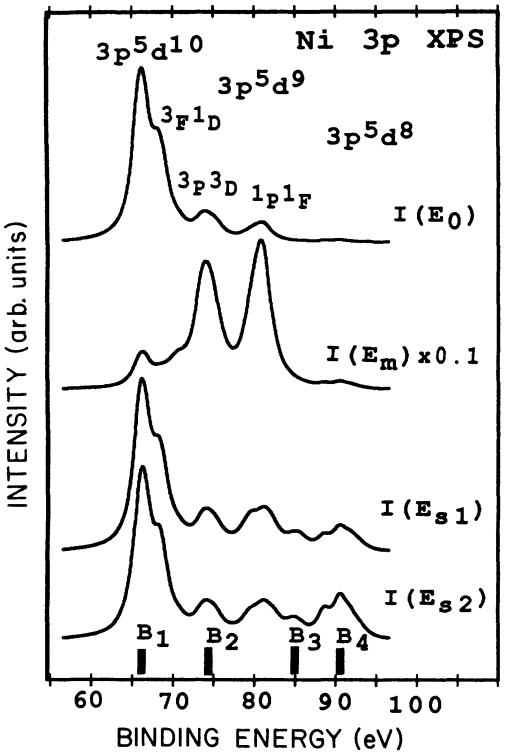

FIG. 2. Calculated Ni $3p$ photoemission intensity at the photon energies E_0, E_m, E_{s1}, and E_{s2} given in Fig. 1.

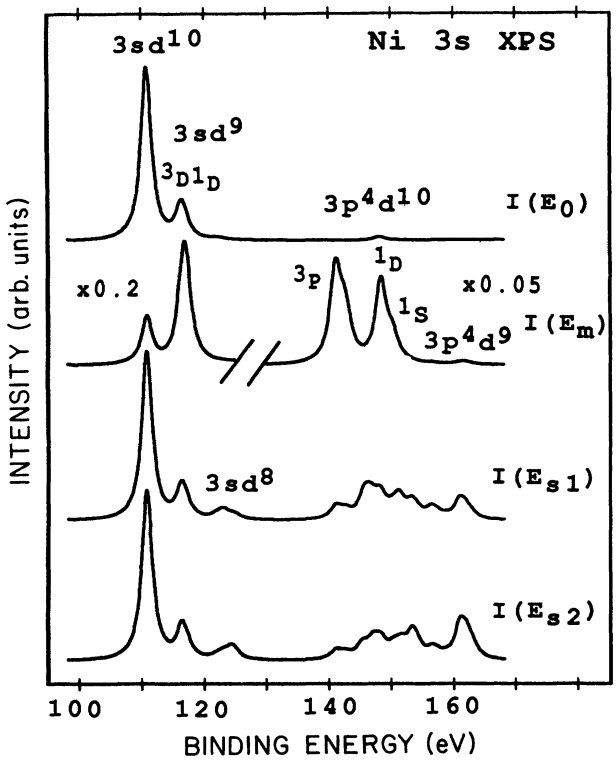

FIG. 3. Calculated Ni $3s$ photoemission and $2p3p3p$ decay intensity at the photon energies E_0, E_m, E_{s1}, and E_{s2}.

interaction with the $3s$ photoemission satellites $3sd^9$ and $3sd^8$, respectively.[12] The $3sd^8$ and $3p^4d^9$ structure is enhanced at E_{s1} and E_{s2} with the weight of the latter spectrum shifted to higher energy. The multiplet splitting of $3p^4$ helps to characterize the spectrum as shown by the difference of the spectra at E_{s1} and E_{s2}.

The $2p$ resonant photoemission of the $3d$ valence band is not given here, but the calculated spectra show a strong resemblance to the experimental results on CuO,[2,12] which is also a mixture of d^8, d^9, and d^{10}. However, the difference between $I(E_{s1})$ and $I(E_{s2})$ is much smaller than in $3p$ photoemission.

We showed that the strong resonant enhancement is of great value for the combined interpretation of the different photoemission spectra. Conversely, we can use the photoemission to analyze the x-ray absorption spectra by collecting the emitted electrons at a constant binding energy (photon energy minus kinetic energy). This is the equivalent of constant initial-state spectroscopy (CIS) in valence-band photoemission. The CIS spectrum integrated over the whole binding-energy range gives the XAS spectrum in total electron yield (Fig. 1). Thus we interpret CIS as partial electron yield at constant binding energy. Figure 1 shows the CIS spectra corresponding to the binding energies B_1, B_2, B_3, and B_4 from Fig. 2. The direct photoemission contribution is shown on the left side. The $\underline{3p}d^{10}$ CIS (B_1) gives a small resonance due to admixture of $\underline{3p}d^9$. The $\underline{3p}d^9$ CIS (B_2) only gives the main absorption line, confirming its $\underline{2p}d^{10}$ character and the $\underline{3p}d^8$ CIS ($B_{3,4}$) shows a very enhanced $\underline{2p}d^9$ satellite structure. The latter confirms the d^8 origin of the $2p$ absorption satellite and shows the increased singlet character at higher energy.

In our example we have omitted Auger transitions to final states with two photoelectrons. These occur above the continuum threshold of the resonance state and give features with constant kinetic energy independent of the photon energy. The Auger intensity becomes weak under similar conditions as the direct photoemission. Thus, we need a resonance with a large ratio between the transition matrix element for x-ray absorption and direct photoemission. More precisely, in a one-level-in-one-continuum model the determining factor is q, the asymmetry parameter of the Fano line shape of the absorption.[1] The enhancement by a specific decay channel is of the order of q^2 times the fraction of the total decay that goes into that channel, so a value of $q=10$ or higher is needed to analyze XAS and XPS satellites with an intensity of a few percent. Such high q values are normal for deep core-level excitations to the d states of transition metals and f states of rare earths and actinides, where the excited state is localized due to the attractive Coulomb interaction between the core hole and the excited electron. This allows the study of valence mixing in these compounds. Applications may be found in CuO-based high-T_c superconductors where the character of the O $1s$ preedge XAS (Ref. 13) and the Cu $2p$ XAS satellite[14] can be analyzed. Also, in $3d$ transition-metal compounds the origin of satellite structures, i.e., polaronic versus charge-transfer screening, can be studied[15] and quadrupole transitions can be sep-

arated from dipole transitions in the $1s$ absorption preedge. For example, the dipole excited state $\underline{1s}d^n4p$ decays to $\underline{2p}d^n$ and $\underline{2p}d^{n-1}$ photoemission states, whereas the quadrupole excited state $\underline{1s}d^{n+1}$ can only decay to a $\underline{2p}d^n$ photoemission state. Likewise, confirmation may be found for the presence of quadrupole transitions in the $2p$ absorption of rare earths, which are predicted in circular dichroism.[16]

In conclusion, excitation at the energy of deeper core levels can enhance specific structures in core-level photoemission by 2 orders of magnitude. This allows a clear assignment of core-level spectra of covalent materials.

[1]L. C. Davis, J. Appl. Phys. **59**, R25 (1986); O. Gunnarsson and T. C. Li, Phys. Rev. B **36**, 9488 (1987).

[2]L. H. Tjeng, C. T. Chen, J. Ghijsen, P. Rudolf, and F. Sette, Phys. Rev. Lett. **67**, 501 (1991).

[3]See, e.g., *Photoemission in Solids I*, edited by M. Cardona and L. Ley (Springer-Verlag, Berlin, 1978).

[4]T. Jo and G. A. Sawatzky, Phys. Rev. B **43**, 8771 (1991); G. van der Laan and B. T. Thole, J. Phys. Condens. Matter **4**, 4181 (1992).

[5]The ground-state weights of nickel are different from previous reported values (Ref. 4) to compensate for the neglect of $3d$ spin-orbit coupling, molecular field, and anisotropic mixing. We used the parameters $E(d^{10})=0$, $E(d^9)=0.75$, $E(d^8)=3$, $Q(2p,3d)=2.5$, $Q(3s,3d)=Q(3p,3d)=4.5$, $Q(3d,3d)=1.5$, $V_{\text{mixing}}=1.8$ eV, $\zeta(3d)=0$ eV. The Slater (reduced to 80%) and core spin-orbit parameters were given by G. van der Laan and B. T. Thole, Phys. Rev. B **43**, 13401 (1991); and G. van der Laan, J. Phys. Condens. Matter **3**, 1051 (1991). The XPS and CIS spectra were broadened by a Lorentzian of $\Gamma=1$ eV. The spectra are calculated treating the excitation to first order in the exciting field and to all orders in the transitions to the continua, by the method used in H. Ogasawara, A. Kotani, B. T. Thole, K. Ichikawa, O. Aita, and M. Kamada, Solid State Commun. **81**, 645 (1992).

[6]S. Hüfner and G. K. Wertheim, Phys. Lett. **51A**, 299 (1975); **51A**, 301 (1975).

[7]C. T. Chen, F. Sette, Y. Ma, and S. Modesti, Phys. Rev. B **42**, 7262 (1990).

[8]Hartree Fock values for the dipole transitions and configuration interactions are obtained using Cowan's code [R.D. Cowan, *The Theory of Atomic Structure and Spectra* (University of California Press, Berkeley, 1981)]: $\langle 2p||r||3d\rangle=-0.17723$ a.u.; $2p3p3d$ decay: $\langle 3p||r||\epsilon_s\rangle=0.001494$, $\langle 3p||r||\epsilon_d\rangle=-0.005667$ a.u./$\sqrt{\text{eV}}$; $R^1_{d,e}(2p,3p;3d,\epsilon_s)=-0.03059$, -0.07587, $R^{1,3}_{d,e}(2p,3p;3d,\epsilon_d)=0.04775$, 0.03731, 0.08783, 0.03303, $R^3_{d,e}(2p,3p;3d,\epsilon_g)=-0.08680$, -0.10264 $\sqrt{\text{eV}}$.

[9]$2p3s3d$ decay: $\langle 3s||r||\epsilon_p\rangle=-0.003251$ a.u./$\sqrt{\text{eV}}$; $R^1_{d,e}(2p,3s;3d,\epsilon_p)=-0.001437$, -0.04867, $R^3_{d,e}(2p,3s;3d,\epsilon_f)=0.03088$, 0.10337 $\sqrt{\text{eV}}$.

[10]$2p3p3p$ decay: $R^{0,2}(2p,3p;3p,\epsilon_p)=0.07226$, 0.03907, $R^2(2p,3p;3p,\epsilon_f)=0.09629$ $\sqrt{\text{eV}}$; $R^1(3p,3p;3s,3d)=19.3468$ eV.

[11]J. F. van Acker *et al.*, Phys. Rev. B **37**, 6827 (1988).

[12]Y. Seino, H. Ogasawara, A. Kotani, B. T. Thole, and G. van der Laan, J. Phys. Soc. Jpn. **61**, 1859 (1992).

[13]P. Kuiper *et al.*, Phys. Rev. B **38**, 6483 (1988).

[14]M. Abbate *et al.*, Phys. Rev. B **42**, 7914 (1990).

[15]G. van der Laan, Phys. Rev. B **41**, 12366 (1990).

[16]P. Carra *et al.*, Phys. Rev. Lett. **66**, 2495 (1991).